energies

MDPI

Article

Acoustic Signature and Impact of High-Speed Railway Vehicles in the Vicinity of Transport Routes

Krzysztof Polak [1,*] and Jarosław Korzeb [2]

[1] Railway Track and Operation Department, Railway Institute, 04-275 Warsaw, Poland
[2] Faculty of Transport, Warsaw University of Technology, 00-662 Warsaw, Poland; jaroslaw.korzeb@pw.edu.pl
* Correspondence: kpolak@ikolej.pl

Abstract: In this paper, an attempt is undertaken to identify the acoustic signature of railway vehicles travelling at 200 km/h. In the framework of conducted experimental research, test fields were determined, measurement apparatus was selected and a methodology for making measurements was specified, including the assessment of noise emission on curved and straight track for electric multiple units of Alstom type ETR610-series ED250, the so-called Pendolino. The measurements were made with the use of an acoustic camera and a 4 × 2 microphone array, including four equipped measurement points and two microphones located at the level of the head of the rail and at a height of 4 m above this level. As a result of the conducted experimental research, the dominant noise sources were identified and amplitude–frequency characteristics for these sources were determined by dividing the spectrum into one-third octave bands in the range from 20 Hz to 20 kHz. The paper also considers issues related to the verification of selected models of noise assessment in terms of their most accurate reflection of the phenomenon of propagation in close surroundings. On the basis of conducted experimental studies, the behaviour of selected models describing the change of sound level with frequency division into one-third octave bands as a function of variable distance of observer from the railway line on which high-speed railway vehicles are operated was verified. In addition, the author's propagation model is presented together with a database built within the scope of the study, containing the actual waveforms in the time and frequency domain.

Keywords: railway noise; high-speed railways; environmental impact

Citation: Polak, K.; Korzeb, J. Acoustic Signature and Impact of High-Speed Railway Vehicles in the Vicinity of Transport Routes. *Energies* **2022**, *15*, 3244. https://doi.org/10.3390/en15093244

Academic Editors: Larysa Neduzha and Jan Kalivoda

Received: 9 March 2022
Accepted: 25 April 2022
Published: 28 April 2022

1. Introduction

According to the European Environment Agency report [1] results, railway transport is the second-largest source of noise in Europe. It affects about 4% of the population during the day–evening–night period and 3% during the night. Almost 22 million people are exposed to noise intensity of at least 55 dB during the day–evening–night period and about 16 million people to noise at night (of intensity of minimum 50 dB). The scale of this phenomenon is influenced by a number of factors, including the technical condition of the railway superstructure and rolling stock, landforms and land use, and the high speed of railway vehicles [2,3].

The share of high-speed railway vehicles in the rolling stock of operators providing public transport services is continuously increasing. At present, in Poland, on railway lines with the highest speed, there may operate Alstom type ETR610 series ED250 vehicles (the so-called Pendolino). These vehicles can travel at a maximum speed of 250 km/h; however, due to technical limitations of the railway infrastructure, their maximum operating speed on the Central Railway Line (railway line no. 4 Grodzisk Mazowiecki-Zawiercie) is equal to 200 km/h [4].

The literature analysis showed that there are many works and studies aimed at identifying or determining the acoustic signature of railway vehicles [5–12]. The authors of this work carried out tests in accordance with the methodology specified in the ISO 3095

standard [13]. According to the standard [13], measurements should be made at one or two measurement points, with one microphone in each. The measurement points should be located at a distance of 7.5 m from the track axis at a height of 1.2 m from the rail head and/or at a distance of 25 m at a height of 3.5 m from the rail head.

These tests mainly involved high-speed vehicles travelling at speeds exceeding 200 km/h [11,14–16]. In addition, a review of literature publications and studies conducted so far in Poland reveals a lack of available studies on the characteristics of the dominant noise sources generated by Alstom ETR610 series ED250 high-speed railway vehicles. In this study, measurements were made not only to examine the noise level of the train passage, but an attempt was made to identify the acoustic signature as accurately as possible, hence a nonstandard location of the measurement points was proposed.

External rail noise may arise from a number of sources, including rolling noise, impact noise, traction noise, aerodynamic noise or braking and starting noise. The noise of a particular unit depends, among other things, on the design of the unit and the operating conditions, and therefore a characterisation of the noise emission of the unit is an important element in minimising the acoustic impact [13].

In this article, selected results and conclusions were discussed from experimental research conducted with the use of an acoustic camera and a 4 × 2 microphone array (four measurement points at a distance of 5 m, 10 m, 20 m and 40 m from the track axis, two microphones located at the height of the rail head and at a height of 4 m from the rail head). The aim of this paper is to characterise the acoustic signaling of high-speed railway vehicles travelling at 200 km/h in Polish conditions. The main sources of noise generation were identified and their spectrum described by amplitude–frequency characteristics. Such an approach is nonstandard due to the tertial resolution of the identified propagation characteristics. Acoustic signals coming from the studied object were measured, for which no complex work has been carried out so far to assess their acoustic impact on the surroundings. Recognition of the acoustic signature of high-speed railway vehicles will allow for the building of a model of the source of acoustic impacts typical for the analysed vehicles. Due to the very good condition of the track in the studied area and commissioning of the first section admitted to traffic at high speed, it was possible to build a reference source of impact for the purposes of noise modelling as well as to establish the reference threshold against which passes of trains operating with a higher degree of wheel wear or on tracks with a higher degree of rail wear can be evaluated in the future.

Such information can be used to establish the relationship between environmental impacts and the technical condition of the rolling stock in operation. Complementing the knowledge on their acoustic impact on the surroundings will allow more effective work on minimising the negative impact of noise generated by this type of vehicles.

The experimental investigations carried out and the database built within the framework of the study, containing real waveforms in the time and frequency domain, served as a source of information on the generated impacts for the purposes of modelling noise propagation in close surroundings. Selected models of railway noise evaluation were analysed in terms of their most accurate reflection of the propagation phenomenon. On the basis of conducted experimental studies, the behaviour of selected models describing the change of sound level in the *i*-th frequency band as a function of variable distance of the observer from the railway line on which high-speed railway vehicles are operated was verified.

Additionally, on the basis of the obtained measurement results, an own model of noise propagation in one-third octave bands within the audible band (20 Hz–20 kHz) was built, which was characterised by the best accuracy of reflecting the phenomenon of noise propagation in the range of measurement results in particular measurement points and beyond them.

2. Materials and Methods

2.1. Technical Specification of the Research Objects

The objects of the experimental research were Alstom's railway vehicles type ETR610-series ED250-Pendolino (Figure 1). These vehicles are managed by the largest operator in Poland, PKP Intercity S.A. These are bidirectional electric multiple units consisting of seven sections, including four engine sections (two end sections on both sides) and three trailer sections [17,18].

Figure 1. Object of the research: an Alstom vehicle ETR610-series ED250-Pendolino [photo: own elaboration].

Normal-gauge vehicles (suitable for operation on tracks with a gauge of 1435 mm) are equipped with eight asynchronous, three-phase traction motors with a power of 708 kW each. The length of the vehicle is 187.4 m and its weight is 395.5 tones [19]. The vehicles use two-axle bogies with one driving axle and one rolling axle, with a very low mass value and equipped with torsion dampers, which ensure appropriate dynamic characteristics of the vehicle on curves at speeds of 250 km/h [17,20,21].

There were two sections of a railway track selected for the purpose of the experimental research (straight section and curved section), located on the railway line no. 4 Grodzisk Mazowiecki–Zawiercie (Central Trunk Line–CMK), section Grodzisk Mazowiecki–Idzikowice, which is an electrified and mostly double-track line, with maximum design speed of 250 km/h (Figure 2) [22]. Details of the study sites are described, among others, in [2].

Figure 2. Railway track on the 18 + 600 km area of experimental research (a curve).

2.2. Methodology of the Conducted Research Area

The measurements of acoustic signals were conducted on railway line no. 4 Grodzisk Mazowiecki–Zawiercie, section Grodzisk Mazowiecki–Idzikowice, in two locations:

- curved section (R = 4000 m)—approx. 18 + 600 km (loc. Świnice, Długa str.);
- straight section—approx. 21 + 300 km (loc. Szeligi, Dojazdowa str.).

The registration of acoustic events from high-speed railway vehicles was made with the use of measurement apparatus, consisting of the following devices:

- acoustic camera Noise Inspector Bionic M-112;
- two Svantek sound-level meters SVAN 979;
- Svantek four-channel sound-level meter SVAN 958A;
- two Svantek sound-level meters SVAN 955;
- measurement microphones (electroacoustic transducers) from Svantek—8 pieces;
- Svantek 1st class acoustic calibrator SV 36;
- speedometer;
- weather station from Davis Instruments Vantage Pro2.

Detailed information concerning e.g., location of the testing ground, weather conditions, is described in the publications [2,3].

During noise measurements with a microphone array (4 × 2), eight measurement microphones operating in the audible band were used. The microphones were placed at a height of 4 m (from the rail head) and at the rail-head height (approx. 0.8 m from the ground). Additionally, in order to locate the main sources of noise, an acoustic camera located about 20 m from the track axis was used. A schematic of the measurement cross-section during the conducted experimental research is shown in Figure 3. The results obtained were subject to acquisition using Svantek's dedicated software, SvanPC++, which enabled the generation of data for further analysis and processing, as intended. The measurement of noise with a microphone array was performed using the continuous method, i.e., all acoustic phenomena were measured during the experimental studies of each run, while the frequency spectrum was analysed in one-third octave bands for each second. Registration of individual journeys (type of vehicle, time) made it possible, in the further part of the work, to select only the passages of the tested object. A schematic of the measurement path using the microphone array is shown in the diagram (Figure 4).

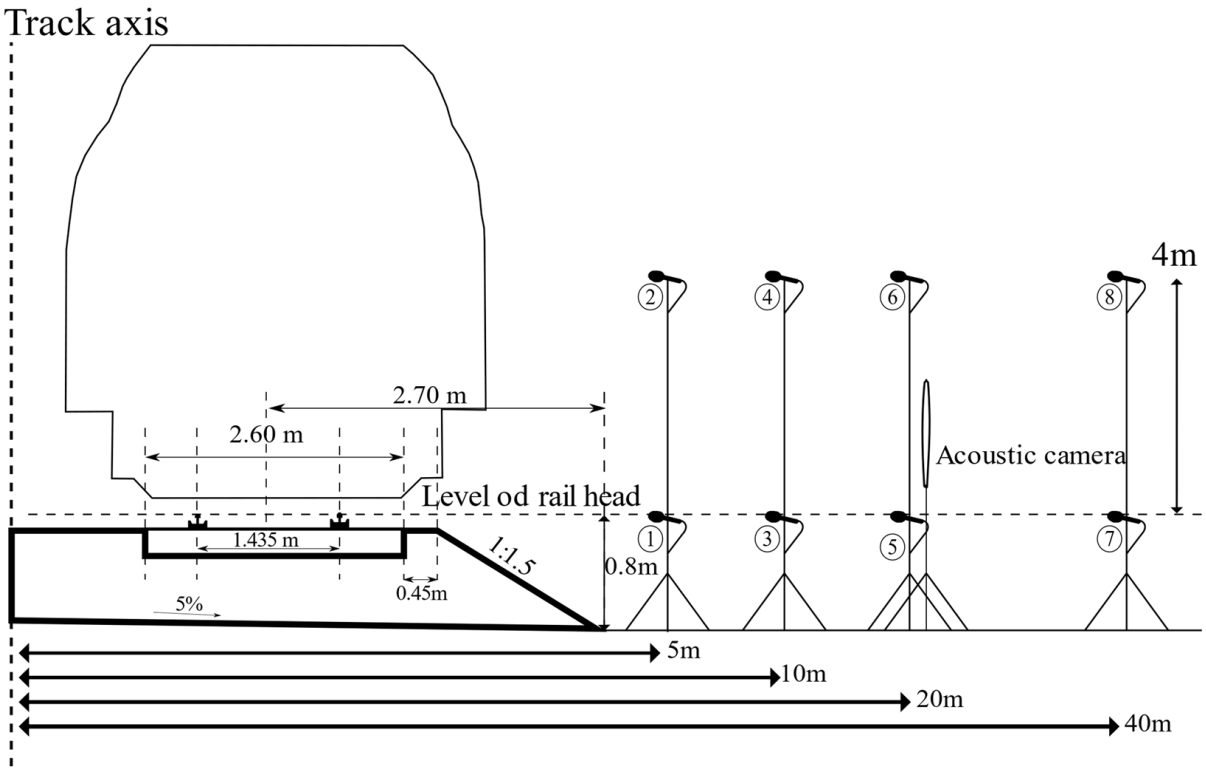

Figure 3. Instrumented cross section during experimental testing [Source: own elaboration].

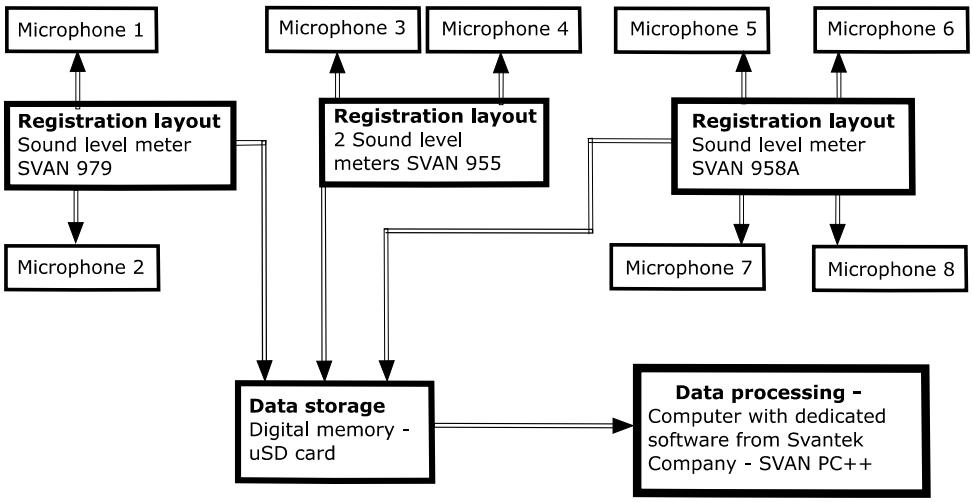

Figure 4. Scheme of the measurement circuit carried out with the sound-level meters [source: own elaboration].

3. Results and Discussion

As a result of the experimental study, the acoustic signature of high-speed vehicles operating in Polish conditions was identified by indicating the main sources of noise generated by the test object using an acoustic camera and obtaining a time history recorded for each pass of the tested vehicle separately (with a step of 1 s), containing the equivalent continuous sound level L_{Aeq} for each second of the pass and obtaining the frequency spectrum of noise for each second, divided into one-third octave bands within the audible band, i.e., from 20 Hz to 20 kHz.

3.1. Identification of Main Noise Sources

A Noise Inspector Bionic M-112 acoustic camera equipped with 112 directional microphones was used to determine the main noise sources. Thanks to the mounted optical camera, the image is assigned to the distribution of acoustic pressure levels. The acoustic camera uses, among others, the beamforming method for measurements, which allows results to be obtained in the frequency range of 400 Hz to 24 kHz, with a sampling rate of approximately 12 Hz.

The beamforming method consists in processing a spatial-temporal signal recorded by a microphone array. Each microphone of the acoustic array, having a specific position relative to its centre, is assigned a time delay which allows it to focus the signal beam in the direction of acoustic wave propagation [5,19,23–27]. By using a time delay, the measured signal is the same for all microphones used. The signal received by the microphones, delayed by an appropriate amount of time, is summed at the output of the array and thus amplified compared to a measurement with only one microphone [25,27–29].

On the basis of the target measurements carried out in August 2019, the main source of noise generated by high-speed railway vehicles travelling at around 200 km/h was defined. In order to better illustrate the results obtained, the acoustic events [dBA] characterised by the highest noise levels were grouped into three frequency ranges, i.e., 500–1000 Hz, 1000–2000 Hz and 2000–3000 Hz (Figure 5).

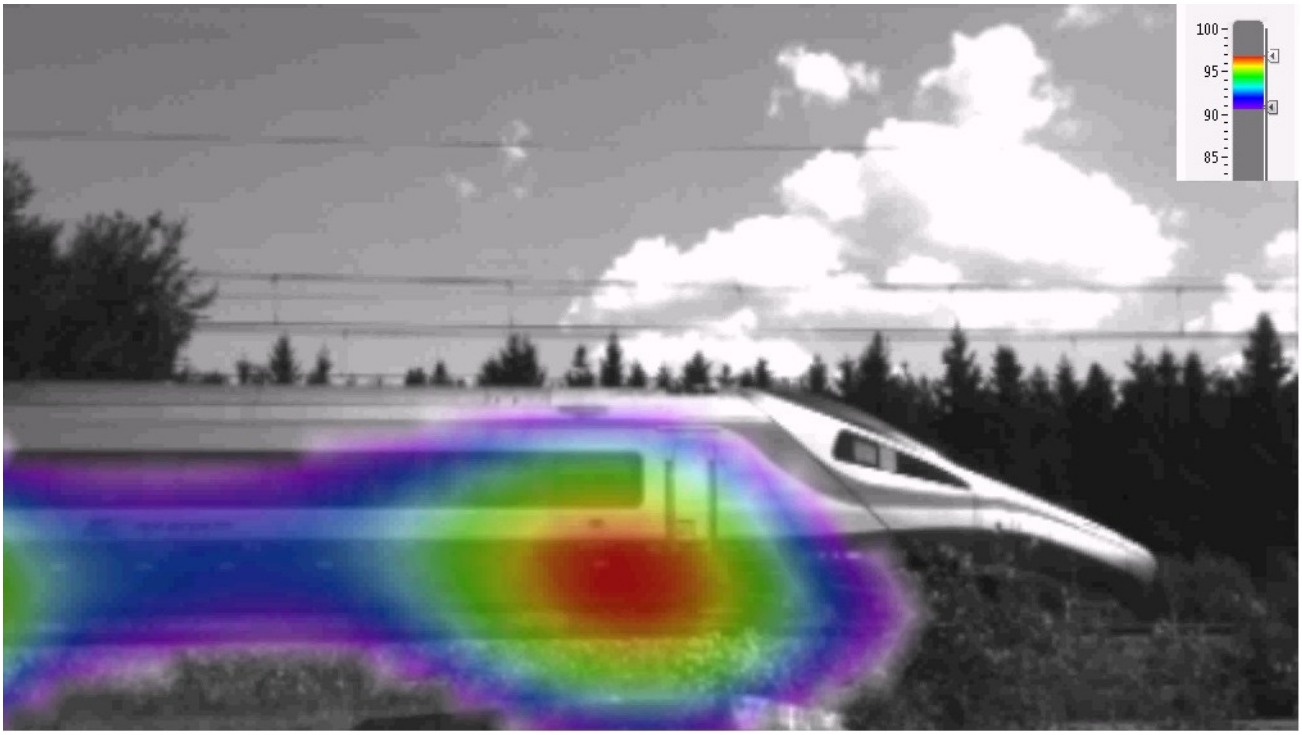

Figure 5. Sound-level distribution in the frequency range 500–1000 Hz—straight section [dBA].

On the basis of experimental tests carried out with the use of an acoustic camera, the main sources of noise [dBA] coming from high-speed vehicles moving on a straight section and along a curve at a speed of 200 km/h were identified. As a result of the experimental studies, it was indicated that the noise resulting from contact phenomena at the wheel–rail interface (rolling noise) and from the operation of drive units are the dominant sources of sound in the frequency range of 500–3000 Hz.

3.2. Noise Propagation in the Immediate Vicinity

In the framework of conducted experimental research, 20 passes of high-speed railway vehicles were obtained for a straight section and a curve, from which the 10 most authoritative results were selected, for which eight signals (acoustic pressure levels–[dB]), 20 s long, were obtained in 31 one-third octave bands from 20 Hz to 20 kHz in two measurement cross sections (straight section and curve). In addition, the equivalent continuous sound level [dBA] was measured at all points in the measurement cross section. The obtained data were subjected to further detailed analysis.

As a first step, the obtained data were verified in order to extract representative acoustic signals [dB] generated by high-speed railway vehicles from the recorded 20-s passes. According to relation (1), the total time of passage of the tested object through the measurement cross section (t) was determined, which amounted to about 3.4 s.

$$t = \frac{l}{v} \tag{1}$$

A representative sample of acoustic signals from speeding vehicles was assumed to be 4 s, which was also confirmed by the results obtained (Figure 6).

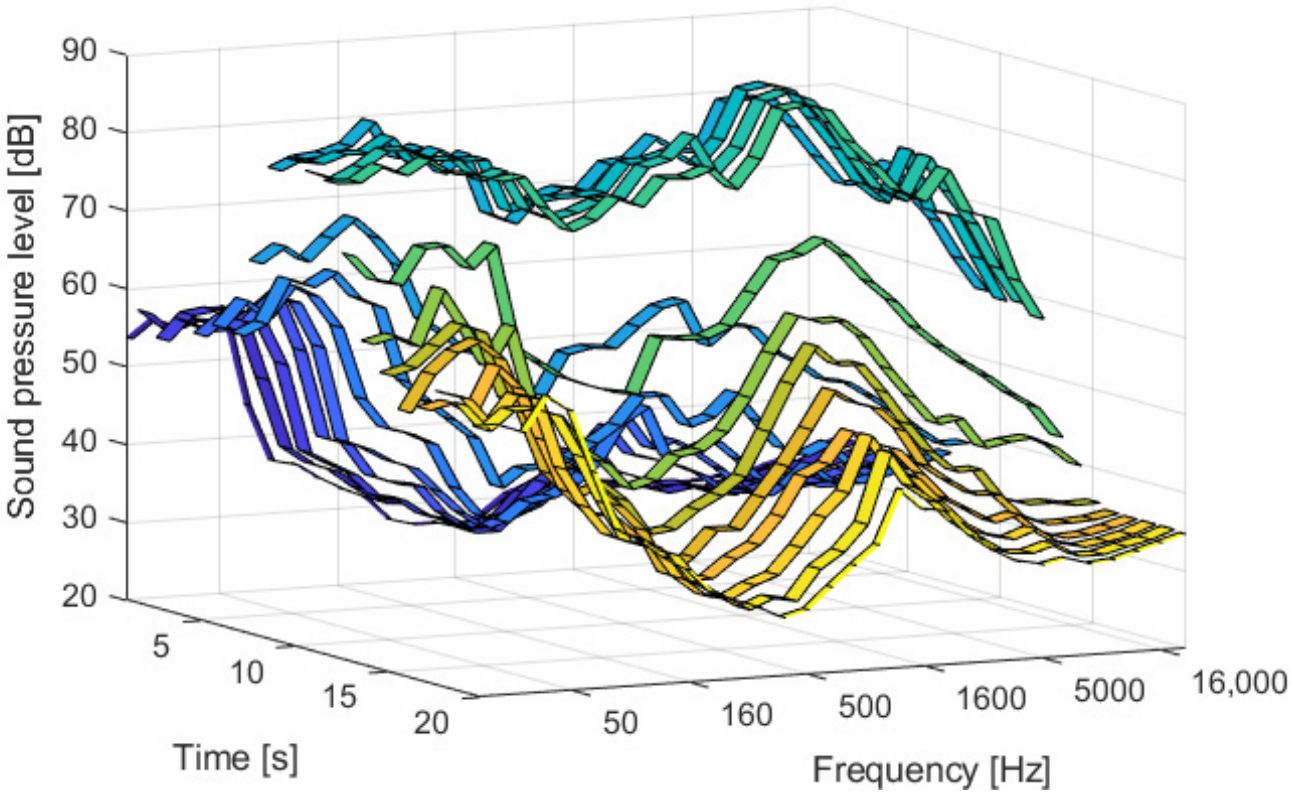

Figure 6. Amplitude–frequency distribution of acoustic pressure levels for a 20-s passage on the straight section.

The analysis made it possible to obtain 4-s passes representative of high-speed railway vehicles travelling on a straight section and a curve. On the diagram below (Figure 7) the distribution of acoustic pressure levels for a selected representative passage (4 s) is shown.

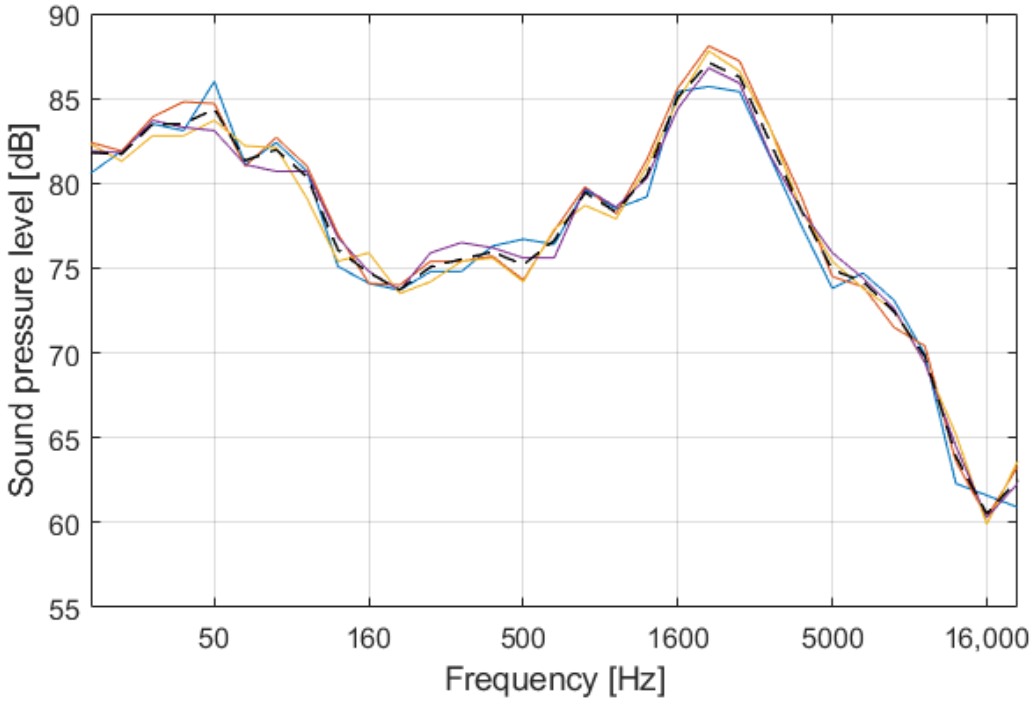

Figure 7. Distribution of acoustic pressure levels for 4 s representative passages on the straight section.

The standard deviation of the sample was then determined on the basis of the obtained data from the representative samples, which show the dispersion of the acoustic pressure levels for the analysed high-speed railway vehicle crossings on the straight section and the curve depending on the tertiary band. The in-sample standard deviation (2), which is the square root of the in-sample variance, was determined according to the formula [30–32]:

$$s = \sqrt{s^2} = \sqrt{\frac{\sum_{i=1}^{N} (\overline{x}_i - x)^2}{n-1}} \quad (2)$$

An example of the distribution of the standard deviation for a selected journey is shown in Figure 8.

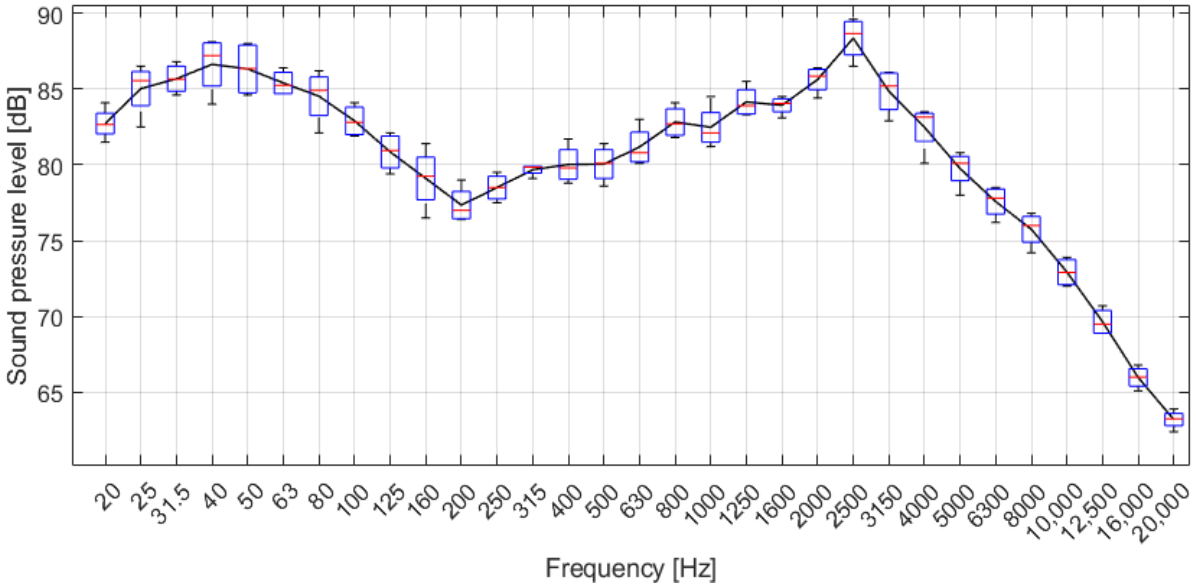

Figure 8. Distribution of standard deviation for a selected straight-section passage.

The analysis of obtained standard-deviation data showed that differences in acoustic pressure levels in given one-third octave bands in most cases did not exceed 2 dB—97.4%; only 2.6% of data indicated exceedances above 2 dB. Exceedances above 2 dB concerned 13 cases out of 496, which were within the range from 2.1 dB to 2.7 dB.

Taking into account that the values of perceived changes in acoustic pressure levels by the human ear vary from 2 dB [31] to 3 dB [33] (depending on the predisposition of the recipient), it was possible to consider the results as reliable.

In order to verify which one-third octave bands' frequencies have the highest acoustic pressure levels, the average spectra of the sound pressure levels were determined for the tested railway vehicle at the level of the head of the rail and at a height of 4 m from the level of the head of the rail, which moved along a straight section and a curve. The average acoustic pressure levels in one-third octave bands at rail-head height for a straight section are shown in Table 1 and Figure 9.

Table 1. Average acoustic pressure levels [dB] in one-third octave bands at rail-head height for a straight section.

One-Third Octave Bands [Hz]	5	10	20	40
20	99.8	95.4	94	89.7
25	99.8	96.6	94.3	90.9
31.5	100.6	97.1	95.1	91
40	101.4	98.3	95.9	92
50	102	99.1	96.3	92.6
63	100.5	100	94.9	91.2
80	100	98.5	94.3	89.9
100	98.3	97.9	93.6	89.6
125	96	95.1	91.4	85.4
160	93.2	92.5	90.7	83.7
200	91.6	90.5	88.3	81.4
250	93.3	89.4	85.8	79.2
315	94.1	88.4	83.3	76.7
400	94.2	87.3	82.5	75.7
500	95	88	83.5	77.3
630	95.9	90.2	85.2	77.6
800	97.9	93.9	87.4	79.8
1000	96.5	94.5	87.9	80.5
1250	97.4	95.2	88.8	81.2
1600	100.3	98.5	92.7	86.9
2000	101.6	99.7	95.4	88.1
2500	103	100.1	93.8	87.1
3150	99.8	97.3	89	86.3
4000	96.6	93.4	84.5	80.4
5000	93.8	90.1	80.7	77
6300	92	87.7	77.6	72.6
8000	91.6	87.4	76.5	68.9
10,000	88.4	84.4	71.5	65.1
12,500	84.8	80	66.4	58.7
16,000	80.7	75.6	57.5	55.2
20,000	78.1	70.2	54.6	58.3

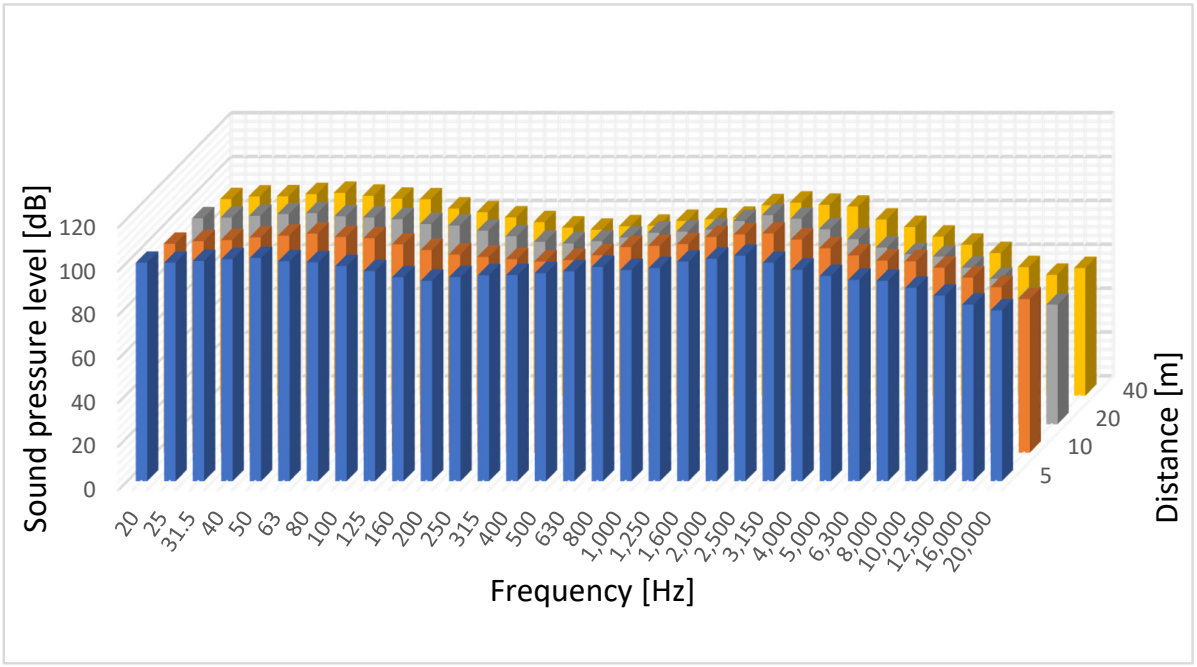

Figure 9. Average acoustic pressure levels in one-third octave bands at rail-head height for a straight section.

For both situations studied (straight section and curve), at the level of the rail head in the close vicinity of the railway line (at a distance of 20–40 m from the track centre), the low bands between 20 Hz and 200 Hz are dominant, with levels ranging from 88.3 dB to 96.9 dB. In the case of medium-frequency bands for the straight section and curve, at a distance of 20–40 m, high values of acoustic pressure levels were recorded for frequencies from 1600 Hz to 3150 Hz (89.0 dB–96.9 dB). In addition, for a railway line located on a curve, high acoustic pressure levels were recorded for frequencies between 630 Hz and 1250 Hz (89.6 dB–95.0 dB).

For measurement points located 4 m from rail-head level (at a distance of 20–40 m), the highest acoustic pressure levels are seen in the low bands from 20 Hz to 100 Hz and the medium bands, i.e., from 500 Hz to 3150 Hz.

In addition, the research carried out has shown that for the passage of high-speed vehicles along a curve with a radius of approximately R = 4000 m, the dominant frequencies characterising the passage of a high-speed railway vehicle can be identified.

Based on the analysis of the differences in acoustic pressure levels (difference of more than 3 dB) for individual one-third octave bands (for the observation point at the level of the rail head), it should be noted that in the case of high-speed railway vehicles travelling along a curve, higher values were recorded for bands in the range of 315 Hz to 2000 Hz (difference of 3 to 10.8 dB). In very close proximity to the railway line (5 m), the dominant characteristics are also 80 Hz, 100 Hz, 16,000 Hz and 20,000 Hz, for which the maximum differences with respect to the straight section range from 4.3 dB to 5.3 dB. In case of the observation point at 4 m above rail-head level, individual differences ranging from 3.3 dB to 8.1 dB were recorded. The fairly evenly distributed acoustic pressure levels at 4 m above rail-head level indicate that rolling noise is the dominant noise source for railway vehicles travelling at 200 km/h.

Taking into consideration that more than 97% of standard deviation results—representing the scatter of acoustic pressure levels between the measurement series for a given one-third octave band—did not exceed 2 dB, the average frequency spectra of acoustic pressure levels were determined. In order to compare and present the results of the average spectra of the effect signals, the exposure acoustic pressure levels (dB) were determined for particular ranges of the one-third octave bands. The exposure acoustic pressure levels for the straight

section and curve at four measurement points, located at distances of 5 m, 10 m, 20 m and 40 m from the track axis (Figures 10 and 11), were calculated according to the relation [34]:

$$L_{EK} = \left[\frac{1}{n} \sum_{i=1}^{n} 10^{0,1 L_{Eki}} \right] \quad (3)$$

where:

- L_{EK}—exposure level of the acoustic pressure [dB];
- L_{Eki}—level of the acoustic pressure in the n-th one-third octave band [dB].

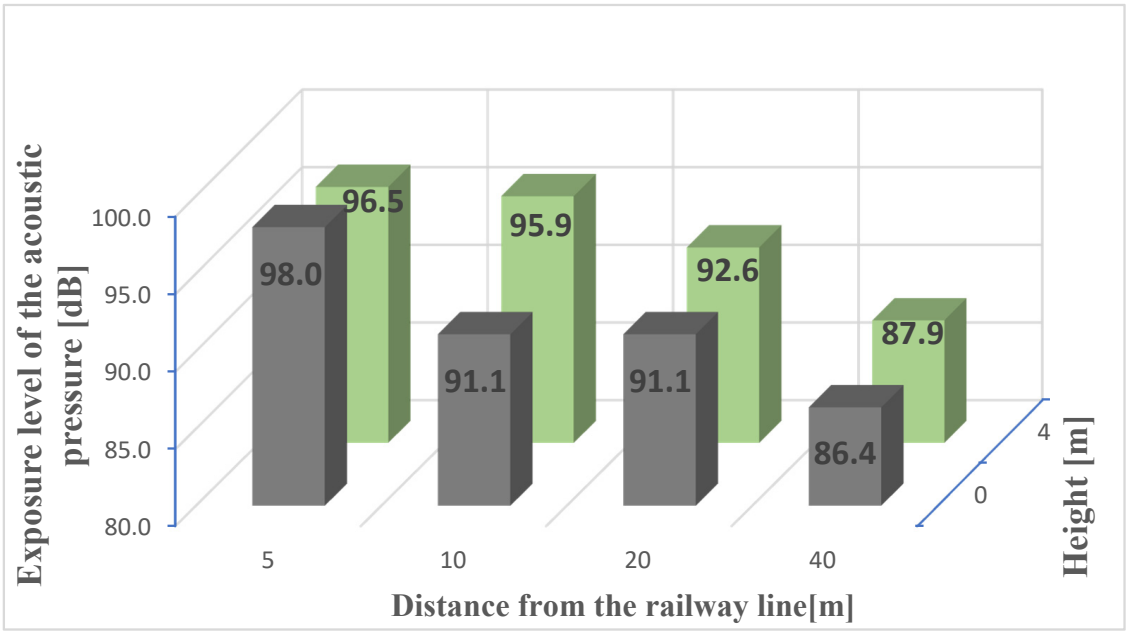

Figure 10. Exposure acoustic pressure level for a straight section at rail-head level (0 m) and at 4 m from rail-head level.

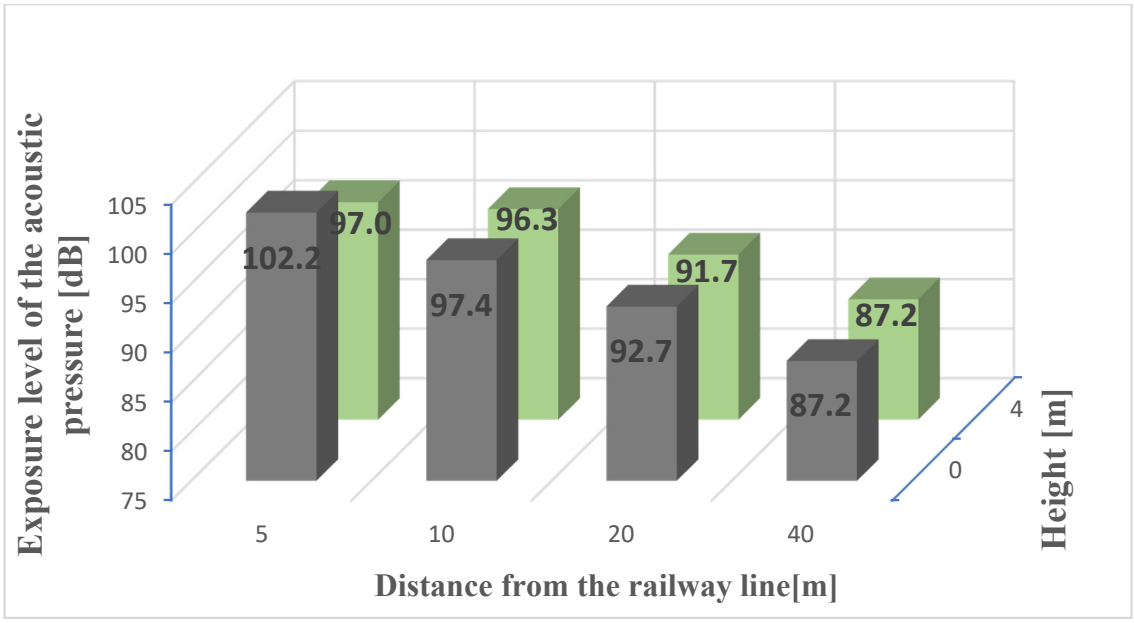

Figure 11. Exposure acoustic pressure level for a curve at rail-head height (0 m) and at 4 m from rail-head height.

The exposure acoustic pressure level at 4 m above rail-head level for high-speed vehicles travelling on a straight section and on a curve is very similar for all distances studied. The differences between the values obtained did not exceed 1 dB, indicating a very similar energy composition in both test cases.

At the level of the rail head (0 m) for the straight section and the curve, at distances of 20 m and 40 m, there were no great differences in the exposure levels (from 0.8 dB to 1.6 dB), which indicates a similar distribution of results. Significant differences in amplitude of exposure acoustic pressure level were recorded between straight and curved section (at the rail-head level) for close distances from the railway line (5 m and 10 m from the track axis), for which the divergence in levels was, respectively, 4.2 dB and 6.3 dB. This situation may be indicative of an increased rolling noise contribution due to the additional friction of the lateral surface of the wheels against the rail.

3.3. Model of Sound Propagation

The construction of the sound-propagation model began with the verification of the batch data. The data obtained from the 4 × 2 microphone array were verified by determining the correlation coefficient for all 4 s pairs of representative passages. The standard Matlab-*corrcoef* high-level language command was used to determine the correlation coefficients for all the mentioned above pairs. The correlation coefficient is defined as the quotient of the covariance and the product of the standard deviations of the variables under consideration and is determined in accordance with the relation shown in Equation (4) [35,36].

$$\mathrm{P}(A,B) = \frac{cov\ (A,B)}{\sigma_A \sigma_B} \tag{4}$$

For about 99% of the cases, the calculated values of the correlation coefficient were not lower than 0.80. The maximum values of the correlation coefficient for the straight section and the curve were equal to 0.998 and 0.999, respectively. In the case of minimum coefficient values, the values were equal to 0.431 for a straight section and 0.753 for a curve. After a preliminary analysis of the obtained data, only the crossings with the highest correlation coefficients were selected for further considerations.

The resulting spectral levels in the one-third octave band of acoustic pressure levels and equivalent continuous sound levels from 10 high-speed rail-vehicle passages were used to determine statistical parameters that provided input data for the propagation models studied. Statistical parameters were defined for each distance from the track centre (i.e., 5 m, 10 m, 20 m, 40 m). The analysis was performed separately for each tested height, i.e., at the level of the rail head and 4 m above the rail head, separately for each measurement cross section (straight section and curve). In order to determine the average level and distribution of values, statistical measures were determined on the basis of representative passages (4 s) in the form of a median, which was calculated on the basis of the relation [35,36]:

$$\mathrm{Me} = \begin{cases} \frac{x_{N+1}}{2}; & \text{when N is an odd number} \\ \frac{x_{\frac{1}{2}N} + x_{\frac{1}{2}N+1}}{2}; & \text{when N is an even number} \end{cases} \tag{5}$$

Based on the obtained batch data, four selected models of railway-noise assessment were analysed in terms of their degree of reflection of the propagation phenomenon. Results of conducted experimental research were used to verify behaviour of particular models describing change of sound level in the *i*-th frequency band as a function of variable distance of observer from the railway line on which high-speed railway vehicles operate.

Four models were verified:

- linear (1st degree);
- using a 2nd degree polynomial;
- using a 3rd degree polynomial;
- power model with a free expression.

An example of noise-propagation model fitting for a straight section described by polynomials of 1st–3rd order (W1R, W2R, W3R), based on experimental data is shown in the following diagrams (Figures 12 and 13).

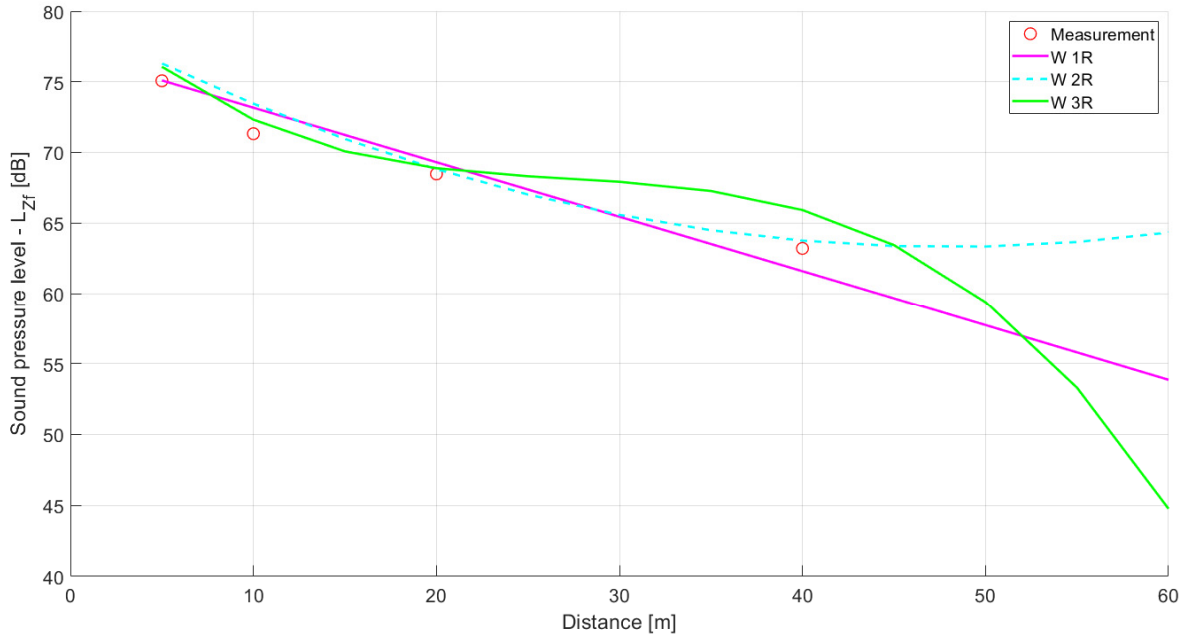

Figure 12. Fitting a 1st–3rd order polynomial noise-propagation model at 250 Hz for a straight section at rail-head level.

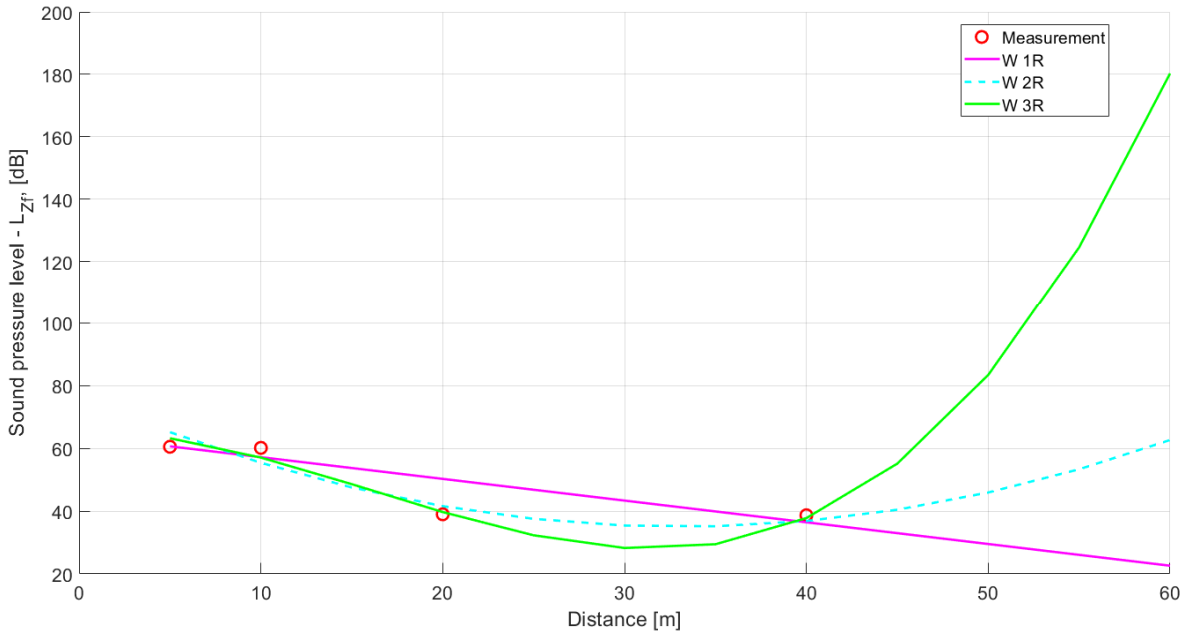

Figure 13. Fitting a 1st–3rd order polynomial noise propagation model at 16,000 Hz for a straight section at rail-head level.

On the basis of the conducted analysis of fitting the noise-propagation model described by polynomials of 1st–3rd order, it may be noticed that all models behave quite well in the range of measurement points (up to 40 m). The obtained characteristics indicate that the linear model, marked in purple on the diagrams, in most cases best represents the results of measurements at specific measurement points, as well as at a distance up to 60 m from the track axis.

The model curves of the 2nd and 3rd degree outside the measurement points are characterised by very large scatter in all ranges of frequency bands and equivalent continuous sound levels. It should be stated that the best representation of the studied phenomena during the passage of railway vehicles at high speeds is a linear model, even though the analysis of characteristics indicates a tendency to too rapid a reduction of noise in the function of distance, beyond the measurement points.

The next step of the study was to verify the representation of the noise-propagation phenomenon using a power model with free expression (FPM). This model takes the form of [37]:

$$L_i = a_i r^{b_i} + c_i \tag{6}$$

where:

- L_i—acoustic pressure level in the i-th frequency band;
- a_i, b_i, c_i—experimental coefficient of the model for t-th frequency band;
- r—distance from sound source.

The final stage of the work was the construction of the author's model using a logarithmic curve.

The evaluation of the tested models showed qualitatively good representation of the measurement results at the selected measurement points. The linear model and the power model with free expression were characterised by the best representation of noise propagation beyond the measurement points. However, they showed a tendency for too rapid a decrease in noise as a function of distance exceeding the distance of the farthest measurement point. Polynomial models of 2nd and 3rd order, outside the measurement points, were characterised by very big errors and unacceptable scattering of results in all ranges of frequency bands and equivalent continuous sound levels.

The author's model, including band noise correction, was also developed and is presented in the study, and was also verified in terms of reproducing the propagation phenomenon. The author's model was characterised by good accuracy for the obtained levels of noise propagation in the range of results obtained experimentally in individual measurement points. Analysis of results obtained for this model—beyond verifiable measurement points, due to the absence of abrupt changes of levels and linear character of decreasing level as a function of further distance—implies high probability of correct representation of the phenomenon of propagation of noise from railway vehicles of high speed by this model. However, it requires further verification in the form of future experimental studies.

Due to the band analysis of the signal in the relation describing the model performance for the i-th frequency band, a correction of the level kpi was introduced for each of the analysed frequency bands (KPM). The relation describing the level for frequency band i at distance x from the sound source is expressed as:

$$L_{xi} = L_{ri} - 10z \log \frac{x}{r} + k_{pi} \tag{7}$$

where:

- L_{xi}—experimentally determined noise level at distance x from the source [dB];
- L_{ri}—sound-level value measured at the reference point r [dB];
- z—source type factor (for a linear source z = 1);
- x—distance of observation point from noise source [m];
- r—distance of reference point from noise source [m];
- k_{pi}—level correction for the analysed i-th frequency band [dB].

In order to implement the scheme of the propagation model for each of the analysed frequencies, an attempt was made to determine the parameters of the models by means of the noise-emission correction curve method in Matlab software by using the command-*lsqcurvefit* (with the following parameters: description function, vector of initial conditions,

distances of measurement points, values of the sound level in the measurement points). The vector of initial conditions was defined as:

$$x_0 = [s(1)\ s(2)] \quad (8)$$

where:

- $s(1)$—noise level at the reference point, *Lri* [dB];
- $s(2)$—frequency-band correction value, *kpi* [dB].

The notation of the function became:

$$fun = @(s,x\_org)\ (s(1) - (10*1*log10(x\_org/5)) + s(2))$$

where *x_org* was the distance vector of measurement points; therefore, code call *lsqcurvefit* (*fun*,*x0*,*x_org*,*y*) returned model parameters each time. The implementation of the Matlab function code *nlinfit* (with parameters: distance vector of measurement points, level values at measurement points, function, vector of initial conditions) allowed the determination of the residue vector and the Jacobian for the nonlinear regression model returned as a matrix and the estimated variance–covariance matrix for the calculated coefficients, or the calculation of the variance for the calculated error component.

The coefficients of the author's model expressed by Equation (6) for the straight section are shown in Table 2.

Table 2. Coefficient values of the author's noise-propagation model for straight section.

Frequency Band [Hz]	Straight Section			
	Rail-Head Level		4 m over the Rail-Head Level	
	L_{ri}	k_{pi}	L_{ri}	k_{pi}
20	93,787	−2539	93,280	−0881
25	83,886	−1302	80,973	−2334
31.5	84,330	−1372	81,341	−2241
40	85,373	−1833	82,482	−2143
50	86,555	−1622	83,016	−2006
63	87,256	−1503	83,276	−2099
80	86,230	−1306	82,747	−1995
100	85,367	−1520	82,383	−1821
125	83,842	−0822	80,865	−1577
160	81,222	−1256	78,744	−1538
200	78,642	−0850	77,625	−1258
250	76,956	−1113	76,530	−1164
315	77,569	−2319	76,662	−1483
400	77,320	−3356	77,054	−1671
500	76,886	−3900	77,805	−1235
630	77,455	−3988	78,788	−1146
800	78,176	−3703	79,415	−1394
1000	81,087	−3202	81,476	−1173
1250	79,912	−2528	81,934	−0613
1600	81,170	−2677	83,766	−0588
2000	84,022	−2291	86,171	−0287
2500	85,353	−2153	88,165	−0385
3150	86,717	−2800	87,037	−0854
4000	83,389	−2522	84,840	−0648
5000	79,897	−3163	80,953	−1246
6300	77,242	−3355	77,234	−2008
8000	74,420	−3992	74,351	−2188
10,000	73,401	−4356	73,220	−2652
12,500	69,884	−4770	68,740	−2810
16,000	65,911	−5444	63,984	−3596
20,000	61,175	−5888	57,827	−4307
L_{AEq}	58,976	−5511	54,284	−3867

The analysis of the author's model of noise propagation and the free-expression model show that both methods are characterised by an accurate representation of results. The runs of models indicate that the free-expression model more accurately reflects the results of measurements at specific measurement points, but the differences in relation to the author's model are within error limits. Detailed analysis of the obtained characteristics indicates that the author's model is characterised by better runs outside the measurement points. The free-expression power model, outside the range of measurement points, tends in many cases to reduce noise too quickly as a function of distance, which was also confirmed by detailed analyses in the third-order frequency spectra for individual passages (Figures 14–16).

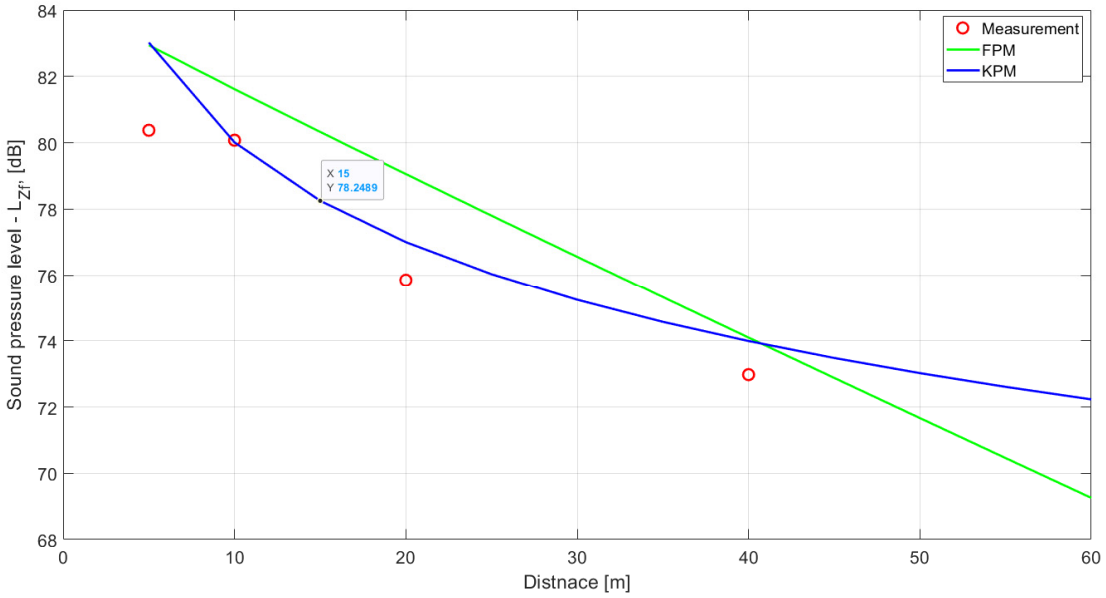

Figure 14. Fitting of the developed noise-propagation model and a free-expression power model for 100 Hz at rail-head level for a straight section.

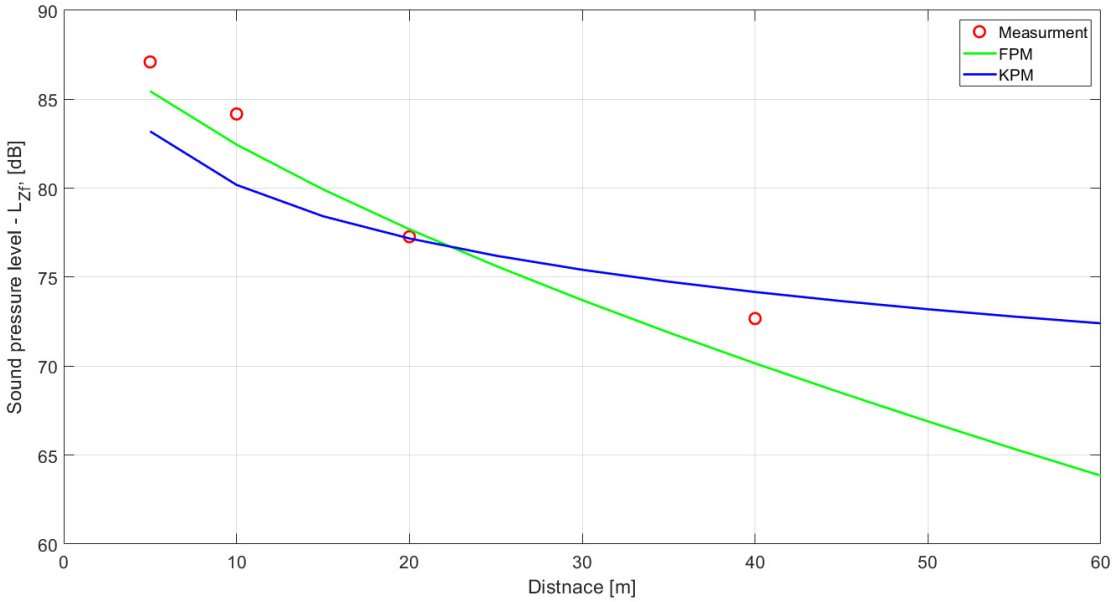

Figure 15. Fitting of the author's noise-propagation model and a free-expression power model for 2000 Hz at rail-head level for a straight section.

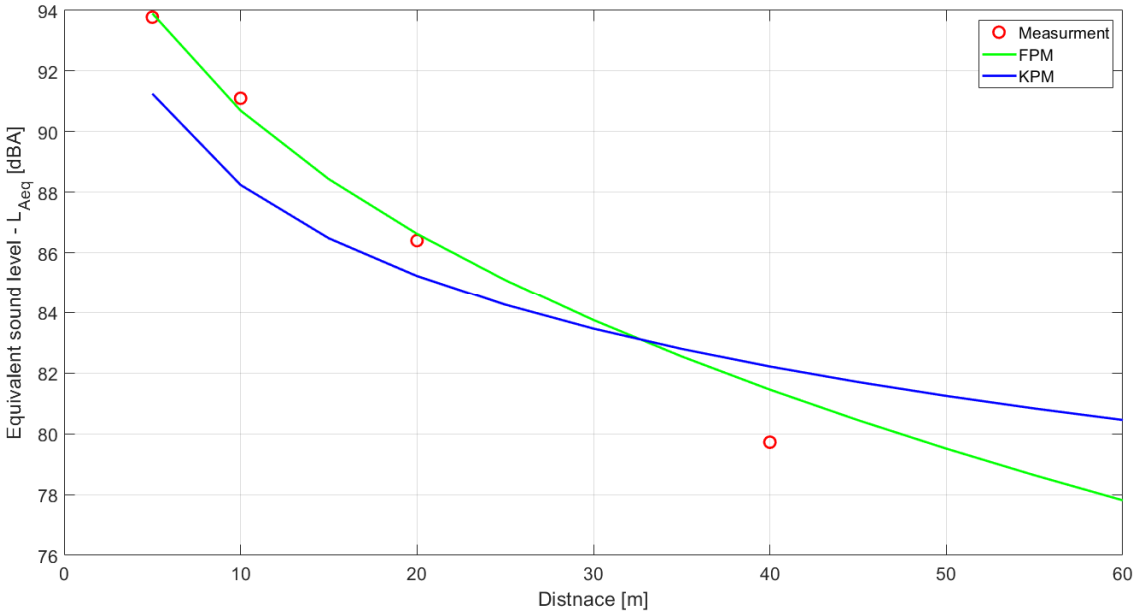

Figure 16. Fitting the author's noise-propagation model and a free-expression power model for the equivalent continuous sound level L_{Aeq}, at rail-head level for a straight section.

4. Conclusions

In the paper, an attempt is made to identify the acoustic signature of a high-speed railway vehicle, moving at a speed of 200 km/h on a straight section and a curve. As part of the experimental research, test fields were determined, measurement equipment was selected, and a methodology for carrying out measurements was specified, including the assessment of noise on a curve and straight line for electric multiple units of Alstom type ETR610-series ED250, the so-called Pendolino. The measurements were made using an acoustic camera and a 4 × 2 microphone array. As a result of the conducted experimental research, the main sources of noise coming from the studied object were identified and the dominant amplitude–frequency characteristics in the range from 20 Hz to 20 kHz, divided into one-third octave bands, were determined.

Additionally, measurements of the equivalent continuous sound level were made for 20-s passes of high-speed railway vehicles, at all points in the measurement cross section. The conducted experimental research made it possible to compare acoustic phenomena recorded separately for a straight section and a curve. The study confirmed that in the case of electric multiple units travelling at 200 km/h, the dominant noise source is the rolling noise resulting from vibrations at the wheel–rail interface. In the case of high-speed railway vehicles travelling along a curve with a radius of about R = 4000 m, the noise resulting from wheel–rail vibrations does not clearly increase the maximum sound levels compared with a straight section.

The highest acoustic pressure levels from high-speed railway vehicles travelling on a straight section, for heights above rail-head level, were recorded in the low (20 Hz to 160 Hz) and medium (1000 Hz to 4000 Hz) bands. For heights 4 m above rail-head level, the highest levels occurred in the range of 20 Hz to 100 Hz (for a distance of 20 m) and 1000 Hz–4000 Hz.

For vehicles travelling in curves, at rail-head level, the highest values were recorded for frequencies in the low bands from 20 Hz to 100 Hz (for a distance of 40 m) and additionally from 125 Hz to 200 Hz (for 20 m) and in the medium bands from 630 Hz to 3150 Hz (for a distance of 20 m). Additionally, at a distance of 40 m, high levels were recorded at 1600 Hz and 2000 Hz. For a height of 4 m above rail-head level, high values of acoustic pressure levels were recorded in the low bands from 20 to 100 Hz (for a distance of 20 m), and for a distance of 40 m in the range of 50 Hz–100 Hz. High values of sound levels were also recorded for the medium bands in the range from 1000 Hz to 3150 Hz.

On the basis of differences in the measured levels of acoustic pressure for the straight section and the curve, the dominant frequencies in the one-third octave bands (at the level of the rail head) characterising the passage of high-speed railway vehicles along a curve of the radius R = ~4000 m were indicated.

Based on the differences in the measured acoustic pressure levels, the dominant frequencies in the one-third octave bands (at the rail-head level) characterising the passage of high-speed railway vehicles over a curve of radius R = 4000 m were identified. Differences in acoustic pressure levels relative to the straight section were recorded for the bands in the range from 315 Hz to 2000 Hz.

Significant differences in amplitude of exposure acoustic pressure level were recorded between the straight section and the curve (at the level of the rail head) for close distances from railway line (5 m and 10 m from track axis). The divergences from the straight section were 4.2 dB and 6.3 dB, respectively, which may indicate an increased contribution of rolling noise due to the additional friction of the lateral surface of the wheels against the rail head.

In this study, results were developed and presented for the author's model including band noise correction, which was also verified to reproduce the propagation phenomenon. The model was characterised by good accuracy for obtained levels of noise propagation in the range of results obtained experimentally in individual measurement points. The analysis of the results obtained for this model (no abrupt changes of levels, linear character of decreasing levels) indicates that there is a high probability of correct representation of the phenomenon of propagation of noise from high-speed railway vehicles by the author's model, also beyond the measurement points.

Detailed recognition of the acoustic signature of high-speed railway vehicles travelling at 200 km/h will make it possible to minimise the acoustic impact more effectively. By identifying the main sources of noise and knowing the dominant amplitude–frequency characteristics of the studied object, it will be possible to optimally select solutions and measures limiting the negative impact of noise on the environment, including appropriate selection of noise barriers (acoustic screens) aimed at the reduction of particular frequency bands. The methodology presented in this paper to carry out experimental studies based on the measurement of acoustic phenomena using an acoustic camera and microphone matrix can also be used for other railway vehicles. Due to the differences in speed and shape of the locomotive/traction unit, it should be assumed that the recognised acoustic signal will have different amplitude and frequency characteristics. Further work directions include carrying out acoustic measurements for other railway vehicles in order to verify and compare characteristics of particular research objects.

Author Contributions: Conceptualisation, K.P. and J.K.; methodology, J.K.; validation, J.K. and K.P.; formal analysis, J.K. and K.P.; investigation, K.P.; resources, K.P.; data curation, K.P.; writing—original draft preparation, K.P.; writing—review and editing, J.K.; visualisation, K.P.; supervision, J.K.; project administration, K.P. All authors have read and agreed to the published version of the manuscript.

Funding: This research received no external funding.

Institutional Review Board Statement: Not applicable.

Informed Consent Statement: Not applicable.

Conflicts of Interest: The authors declare no conflict of interest.

References

1. Peris, E. *Environmental Noise in Europe—2020, European Environment Agency Raport*; European Union: Luxembourg, 2020; No 22/2019.
2. Polak, K.; Korzeb, J. Identification of the major noise energy sources in rail vehicles moving at a speed of 200 km/h. *Energies* **2021**, *14*, 3957. [CrossRef]
3. Polak, K.; Korzeb, J. Measurements of noise from high-speed rail vehicles, Railway Problems. Pomiary hałasu pochodzącego od pojazdów kolejowych zwiększonych prędkości. *Probl. Kolejnictwa* **2019**, *184*, 33–38.
4. Żurkowski, A. Central Trunk Line (CMK) 200km/h. Traffic, timetable and operations. *Tech. Transp. Szyn.* **2015**, *nr 6/2015*, 24–25.

5. Graf, H.R.; Czolbe, C. Pass-by noise source identification for railroad cars using array measurements. In Proceedings of the 23rd International Congress on Acoustics, Aachen, Germany, 9–13 September 2019; pp. 1574–1581.
6. Jiang, S.; Yang, S.; Wu, D.; Wen, B.-C. Prediction and validation for the aerodynamic noise of high-speed train power car. *Transp. Probl.* **2018**, *13*, 91–102. [CrossRef]
7. Li, L.; Thompson, D.; Xie, Y.; Zhu, Q.; Luo, Z.; Lei, Z. Influence of rail fastener stiffness on railway vehicle interior noise. *Appl. Acoust.* **2019**, *145*, 69–81. [CrossRef]
8. Maillard, J.; Van-Maercke, D.; Poisson, F.; Regairaz, J.-P.; Dufour, J.B. Comparison of pass-by railway noise indicators obtained from standard engineering methods with measured values. In Proceedings of the Forum Acusticum, Lyon, France, 7–11 December 2020; pp. 2477–2483. [CrossRef]
9. Uda, T.; Kitagawa, T.; Saito, S.; Wakabayashi, Y. Low frequency aerodynamic noise from high speed trains. *Q. Rep. RTRI* **2018**, *59*, 109–114. [CrossRef]
10. Zea, E.; Manzari, L.; Squicciarini, G.; Feng, L.; Thompson, D.; Arteaga, L.I. Wavenumber–domain separation of rail contributionto pass-by noise. *J. Sound Vib.* **2017**, *409*, 24–42. [CrossRef]
11. Zhang, J.; Xiao, X.; Wang, D.; Yang, Y.; Fan, J. Source contribution analysis for exterior noise of a high-speed train: Experiments and simulations. *Shock. Vib.* **2018**, *2018*, 5319460. [CrossRef]
12. Zhao, C.; Wang, P.; Yi, Q.; Sheng, X.; Lu, J. A detailed experimental study of the validity and applicability of slotted stand-off layer rail dampers in reducing railway vibration and noise. *J. Low Freq. Noise Vib. Act. Control.* **2018**, *37*, 896–910. [CrossRef]
13. *EN ISO 3095*; 2013 Acoustics—Railway Applications—Measurement of Noise Emitted by Railbound Vehicles. CEN: Brussels, Belgium, 2013.
14. Li, M.; Zhong, S.; Deng, T.; Zhu, Z.; Sheng, X. Analysis of source contribution to pass-by noise for a moving highspeed train based on microphone array measurement Measurement. *J. Int. Meas. Confed.* **2021**, *174*, 109058. [CrossRef]
15. Sheng, X.; Cheng, G.; Thompson, D.J. Modelling wheel/rail rolling noise for a highspeed train running along an infinitel long periodic slab track. *J. Acoust. Soc. Am.* **2020**, *148*, 174–190. [CrossRef] [PubMed]
16. Zhang, J.; Xiao, X.; Sheng, X.; Li, Z. Sound source localisation for a high-speed train and its transfer path to interior noise. *Chin. J. Mech. Eng.* **2019**, *32*, 1–16. [CrossRef]
17. Wawrzyniak, A. ETR610 electric multiple units of the ED250 series for PKP Intercity, S.A. Elektrycznepoci ągizespołowe ETR610 serii ED250 dla PKP Intercity S.A. *Tech. Transp. Szyn.* **2013**, *9*, 20–24. (In Polish)
18. Pachla, F. Transmission of vibrations from the ground to the foundation from the movement of passenger trains. *Vibroengineering Procedia* **2019**, *27*, 93–96. [CrossRef]
19. Graff, M. The New Electric Multiple Units for Long-Distance and Regional Traffic in Poland in 2015. *Tech. Transp. Szyn.* **2016**, *nr 1-2/2016*, 22–33.
20. Czarnecki, M.; Witold, G.; Massel, A.; Walczak, S. Introduction of High-Speed Rolling Stock into Operation on the Polish Railway Network. In *High-Speed Rail in Poland: Advances and Perspectives*; Zurkowski, A., Ed.; CRC Press: Warsaw, Poland, 2018; pp. 203–228. [CrossRef]
21. Raczyński, J. The ED250 (Pendolino) Experiences in Poland—First Years of Exploitation, Technika Transportu Szynowego. 2018. no 4/2018. pp. 30–32. Available online: http://yadda.icm.edu.pl/yadda/element/bwmeta1.element.baztech-9b7e36f1-647f-4ee4-aaf5-b0e7d9495dcd/c/Raczynski1TTS4en.pdf (accessed on 22 February 2022).
22. Id-12 (D-29). The List of Lines, Introduced by Order No. 1/2009 of the Management Board of PKP PolskieLinieKolejowe, S.A. of 9 February 2009, as AMENDED., PKP Polskie Linie Kolejowe. 2009. Available online: https://www.plk-sa.pl/files/public/user_upload/pdf/Akty_prawne_i_przepisy/Instrukcje/Wydruk/Id-12_Wykaz_linii_06.2021.pdf (accessed on 22 February 2022). (In Polish).
23. Gade, S.; Ginn, B.; Gomes, J.; Hald, J. Recent advances in rail vehicle moving source beamforming. Instrumentation Reference. *Sound Vib.* **2015**, *4*, 8–14.
24. Le Courtois, F.; Thomas, J.-H.; Poisson, F.; Pascal, J.-C. Genetic optimisation of a plane array geometry for beamforming. Application to source localisation in a high speed train. *J. Sound Vib.* **2016**, *371*, 78–93. [CrossRef]
25. Meng, F.; Wefers, F.; Vorlaender, M. Acquisition of exterior multiple soundsources for train auralization based on beamforming. In Proceedings of the the 10th European Congress and Exposition on Noise Control Engineering, Maastricht, The Netherlands, 31 May–3 June 2015; pp. 1703–1708.
26. Go, Y.-J.; Choi, J.-S. An acoustic source localization method using a drone-mounted phased microphone array. *Drones* **2021**, *5*, 75. [CrossRef]
27. Zhang, J.; Squicciarini, G.; Thompson, D.J. Implications of the directivity of railway noise sources for their quantification using conventional beamforming. *J. Sound Vib.* **2019**, *459*, 114841. [CrossRef]
28. Chiariotti, P.; Martarell, M.; Castellini, P. Acoustic beamforming for noise source localization—reviews, methodology and applications. *Mech. Syst. Signal Process* **2019**, *120*, 422–448. [CrossRef]
29. Polak, F.; Sikorski, W.; Siodła, K. Prototype measurement system for locating sources of acoustic emission-microphone matrix. Poznan University of Technology Academic Journals. *Electr. Eng.* **2015**, *84*, 207–214. (In Polish)
30. Aczel, A.D. *Statistics in Management*, 2nd ed.; PWN: Warszawa, Poland, 2018. (In Polish)
31. Ozimek, E. Sound and its perception. In *Physical and Psychoacoustic Aspects*; PWN: Warszawa, Poland, 2018. (In Polish)
32. Sobczyk, M. *Statistic*; PWN: Warszawa, Poland, 2021; EAN: 9788301151997. (In Polish)

33. Kokowski, P.; Laboratory of Applied Acoustics. *Theoretical Introduction*; UAM: Poznań, Poland, 2003. (In Polish)
34. Ordinance of the Minister of the Environment of 16 June 2011 on the requirements for carrying out measurements of the levels of substances or energy in the environment by the manager of a road, railway line, tramway line, airport or port. *J. Laws* **2011**, *140*, 824.
35. Bobowski, Z. *Selected Methods of Descriptive Statistics and Statistical Inference*; WWSZiP: Wałbrzych, Poland, 2004. (In Polish)
36. Muciek, A. *Determination of Mathematical Models from Experimental Data*; Oficyna Wydawnicza Politechniki Wrocławskiej: Wrocław, Poland, 2012. (In Polish)
37. Borwin, M.; Komorski, P.; Szymański, G. Modeling of the sound propagation for a railway vehicle moving on the track. *Pojazdy Szyn.* **2019**, *3*, 60–68. [CrossRef]